

# Resonant and Nonresonant Hyperpolarizabilities of Spatially Confined Molecules: A Case Study of Cyanoacetylene

Robert Zaleśny,<sup>†</sup> Robert W. Góra,<sup>\*,†</sup> Justyna Kozłowska,<sup>†</sup> Josep M. Luis,<sup>‡</sup> Hans Ågren,<sup>§</sup> and Wojciech Bartkowiak<sup>\*,†</sup>

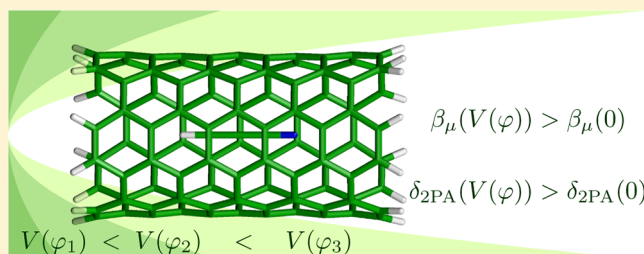
<sup>†</sup>Theoretical Chemistry Group, Institute of Physical and Theoretical Chemistry, Wrocław University of Technology, Wyb. Wyspiańskiego 27, PL–50370 Wrocław, Poland

<sup>‡</sup>Institut de Química Computacional i Catàlisi and Departament de Química, Universitat de Girona, E–17071 Girona, Catalonia, Spain

<sup>§</sup>Department of Theoretical Chemistry and Biology, School of Biotechnology, KTH Royal Institute of Technology, SE–10691 Stockholm, Sweden

## Supporting Information

**ABSTRACT:** In this theoretical study we report on resonant and nonresonant electric-dipole (hyper)polarizabilities of cyanoacetylene molecule confined by repulsive potentials of cylindrical symmetry mimicking a topology of nanotubelike carbon cages. The set of investigated electronic properties encompasses dipole moment, polarizability, first and second hyperpolarizability as well as the two-photon transition matrix elements. The effect of external potential on vibrational contributions to electric-dipole properties is also included in our treatment. The computations are performed at several levels of theoretical approximation including state-of-the-art coupled-cluster (CCSD(T)) and multireference configuration interaction methods (MRCISD(Q)). The results of calculations presented herein indicate that the decrease in dipole moment observed experimentally for the HCCCN molecule solvated in helium nanodroplets may be partially attributed to the confinement effects. The external confining potential causes a substantial drop of the isotropic average electronic polarizability and second hyperpolarizability. In contrast, the vector component of the electronic first hyperpolarizability substantially increases. Nuclear relaxation contributions to all studied electric-dipole properties are found to diminish upon confinement. Our calculations also indicate that the most intense  ${}^1\Sigma^+ \leftarrow \tilde{X}$  one-photon transition is slightly blue-shifted whereas the corresponding oscillator strength is virtually unaffected upon confinement. Interestingly, the absolute magnitude of the diagonal component of the second-order transition moment for the bright state ( $S_{zz}^{0 \rightarrow {}^1\Sigma^+}$ ) increases with the strength of external potential. The effect of structural relaxation on the electric-dipole properties, arising from the presence of the external potential, is also investigated in the present work.



## ■ INTRODUCTION

It is well-established that molecular systems within restricted spaces, as well as under high pressure, possess unusual properties which cannot be observed in unconfined environments. Many aspects of the confinement effects have been recently discussed in special issues of the physical chemistry journals and have also been summarized in collections of review articles.<sup>1–18</sup> In the context of confined species, it is possible to suggest new paradigms for many areas of chemistry and physics including molecular nonlinear optics. New synthetic routes resulted in a plethora of new species, capable of accommodating atoms or molecules: molecular containers, single-walled carbon nanotubes (SWCNTs), fullerenes, porous materials, etc. Recently, it has been shown that the SWCNTs can be used as model high-pressure cells in experimental investigations.<sup>19,20</sup>

It is expected that embedding of a molecule, atom or ion in the confining environment will lead to a perturbation of its electronic density distribution. This, on the other hand, shall be presumably manifested in a variety of linear and nonlinear

optical phenomena (LNLO). Under the assumption that guest molecules retain their separate identities in the considered molecular environment, this effect, to a first approximation, may be described by using a simple analytical confining potential like the penetrable (soft) or impenetrable (hard) box as well as the three-dimensional harmonic oscillator potential.<sup>12,15,17</sup> This concept was first demonstrated by Michels et al. in their theoretical work devoted to the dipole polarizability ( $\alpha$ ) of confined hydrogen atom.<sup>21</sup> Formal models and ab initio calculations play an important role in understanding of the observed phenomena and possibly also in their predictions, especially in the case when experimental studies are difficult or even impossible to carry out. Many follow-up studies confirmed, with the aid of quantum chemistry methods, that both static and dynamic polarizabilities of atoms decrease as a function of increas-

Received: May 17, 2013

Published: June 25, 2013

ing confinement or pressure.<sup>12,13,22–32</sup> Recent studies of the second hyperpolarizability ( $\gamma$ ) of spherically confined hydrogen and helium atoms also indicate similar trends.<sup>30,31</sup> It should be noticed, however, that the opposite behavior has been demonstrated in theoretical studies on (hyper)polarizabilities of atoms under confined Debye plasma and attractive shell potentials (employed to model some of the effects arising from encapsulation in fullerene cages).<sup>32–37</sup> An important picture of the effects of confinement on the electrical response of molecular matter arises from the series of theoretical works by Fowler, Madden, and co-workers.<sup>38–41</sup> Results of calculations for a series of crystalline systems presented in these studies show that the polarizability of an anion in a crystal may be significantly smaller than that of the free ion. Interestingly, the orbital compression directly connected with the spatial confinement must be taken into account in order to quantitatively explain these results. Recently, a gradual decrease of the effective anionic polarizability with the increasing coordination in alkali metal halide clusters was also demonstrated by Zhang et al. based on a combined experimental and computational study.<sup>42</sup> In contrast to atoms, little is still known about the electric-dipole properties of confined molecules. Studies on this subject are limited to a few theoretical works in which various types of confining potentials were included in the molecular Hamiltonian in the form of one-electron operators. The results of such calculations for a set of molecules, encompassing  $\text{H}_2^+$ ,  $\text{H}_2$ ,  $\text{HeH}$ ,  $\text{LiH}$ ,  $\text{NH}_3$ ,  $\text{H}_2\text{O}$ , and  $\text{C}_2\text{H}_4$ ,<sup>24,43–51</sup> allowed to draw a conclusion that even though, similarly as it was observed for atoms, the confinement diminishes the polarizability of the studied species, the dipole moment ( $\mu$ ) exhibits either opposite (e.g.,  $\text{LiH}$  in the cylindrical harmonic potential) or at least a more complicated behavior (e.g.,  $\text{NH}_3$  and  $\text{H}_2\text{O}$  in the hard spherical box).<sup>47,48,51</sup> In more recent studies, performed by some of us, we have employed model potentials combined with accurate electronic structure methods to study both the dipole moment and (hyper)polarizabilities of spatially confined  $\text{LiH}$  molecule.<sup>50,51</sup> Three forms of model potentials were considered, namely a penetrable spherical box, a spherical Pauli-repulsion potential, and a harmonic confining potential. Regardless of the symmetry of employed potential, the first and second hyperpolarizabilities were found to gradually diminish upon increasing the strength of confinement.<sup>50,51</sup> To the best of our knowledge, these studies are still the only theoretical contributions employing various forms of external potentials to estimate the *nonlinear* optical properties of the confined molecules.

An important aspect of confinement that should be highlighted is that the simple “molecule-in-a-box” model reflects the fact that sizes of the cavities and channels are crucial for a proper description of the changes of electronic properties upon incorporation of a guest molecule into the host. It follows from an intuitive picture, arising from the theory of intermolecular interactions, that the orbital compression (deformation) caused by the hard-wall external potential is connected with the valence repulsion.<sup>52</sup> The latter type of interaction is a result of the Pauli exclusion principle and increases rapidly when the wave functions of guest and host molecules start to overlap. Thus, the analyzed models should render qualitatively the effect of confinement on the guest molecule due to the nonpolarizable, electronically inert (hard) environment. This condition, as it has been shown in some studies, is almost fulfilled by the model confining environments represented by aggregates of helium atoms.<sup>53–58</sup> On the other hand, in cases like, for instance, the endohedral complexes, the remaining noncovalent interaction types (electrostatic, induction, and dispersion) are always present.<sup>52</sup> It is well-established that all

of these effects, together with other factors (structural distortion, hydrogen bonding, nonuniform electric fields, charge-transfer processes, etc.), may also contribute to changes of the effective LNLO response of molecules in molecular materials (even under usual external conditions).<sup>56,59–62</sup> It should not be overlooked that there are also alternative theoretical strategies, based on the supermolecular (SM) approximation or the polarizable embedding (PE) schemes, accounting for most of the above effects.<sup>63–71</sup> However, the interpretation of electronic structure of a “super-molecule” might be a difficult task. Particularly since the recent accurate results of calculations for the series of endohedral complexes and 4-nitroaniline in water solvent (some of them are in line with experimental data) indicate that approximate quantum chemical methods (including most of the density functionals) are unable to predict even with qualitative accuracy the stability and the spectroscopic properties of these systems.<sup>72–76</sup> Very good examples of the confined systems, for which theoretical description is extremely complicated, are the endohedral metallofullerenes (EMF). The EMF electronic structure and electrical properties are very often determined by significant metal cluster-to-cage charge-transfer or covalent interactions (see Skwara et al.<sup>77</sup> and the references cited therein).

Unfortunately, there is relatively small number of experimental studies related to the LNLO properties of molecules in the confined spaces, partially due to important objective difficulties connected with their chemical synthesis.<sup>42,78–82</sup> However, some of them are very interesting due to a number of possible applications. Recently, Yu et al. demonstrated a strategy of designing second-order NLO materials by ordered dipolar chromophores confined in the pores of anionic metal–organic framework.<sup>80</sup> Also Kamada et al. and Suzuki et al. discussed a possibility of enhancement of NLO response of dyes confined in interlayer nanospaces of clay minerals.<sup>81,82</sup> It should be also noticed that, in their pioneering studies, Drickamer and co-workers have shown the high-pressure effect on the second harmonic generation (SHG) as well as one- and two-photon-induced fluorescence (TPIF) of various organic materials.<sup>83–87</sup>

The aim of this study is to provide a fundamental understanding of the confinement dependence of the electric properties:  $\mu$ ,  $\alpha$ ,  $\beta$ ,  $\gamma$ , and the second-order transition moment tensor  $S$  (directly related to the two-photon absorption (2PA) strength ( $\delta$ )) of cyanoacetylene (HCCCN) on a molecular scale, in relation to existing knowledge in the field. In doing so we consider external spatial confinement in the form of the harmonic oscillator potential of cylindrical symmetry which mimics a nanotube-like environment. As it was underlined by Patil and Varshni, this form of confining potential is more appropriate in many instances since it is analytical and its increase is gradual.<sup>88</sup> It should also be noticed that such a methodology has been used previously in several theoretical studies devoted to various aspects of molecular and nanoscale physics.<sup>47,51,88–94</sup>

In this study we also investigate the effect of structural relaxation on electric-dipole properties and furthermore the change in vibrational contributions to  $\beta$  and  $\gamma$  upon confinement. The applied formalism allows us to study the relations between electronic structure parameters and the second-order transition moment as a function of the strength of the confining potential. Finally, we will show that the decrease in dipole moment observed experimentally by Stiles et al. for the HCCCN molecule solvated in helium nanodroplets<sup>95</sup> may also be attributed to the confinement effects. To the best of our

knowledge, these important questions have never been considered in the literature.

The reason for selection of cyanoacetylene molecule was twofold. On one hand, HCCCN is an important example of a linear, polar as well as  $\pi$ -conjugated molecule which has been identified in interstellar space and in atmospheres of other astronomical objects.<sup>96–98</sup> This is the rationale behind numerous theoretical and experimental studies on its electronic structure and spectra in the gas phase as well as in the superfluid helium nanodroplets and other rare gas surroundings.<sup>95,99–102</sup> On the other hand, our previous letter on the LNLO properties of the HCCCN molecule, surrounded by helium atoms, reported on the increase of  $\beta$  upon the spatial confinement (in contrast to  $\mu$  and  $\alpha$ ).<sup>55</sup> Its strength was modulated by considering heliumlike nanotubes of three different radii mimicking SWCNTs of (2,2), (3,3), and (4,4) chirality. As already mentioned, this simple model is able to capture the effect arising from Pauli exchange repulsion; yet it included some other, but less important, interaction energy components at the MP2 level of theory. To the best of our knowledge there are no experimental reports about endohedral complexes formed by HCCCN with fullerenes or SWCNTs. However, recent experimental studies have presented successful attempts of encapsulation of other  $\pi$ -conjugated (nonpolar) linear polyynes into SWCNTs.<sup>103–105</sup> As rightly pointed out by Nishide et al. and as we shall discuss further, an encapsulation of linear carbon molecules inside SWCNTs is a promising route to study their optical and electronic properties, as these compounds are difficult to isolate.<sup>104</sup>

## ■ COMPUTATIONAL METHODS

Since our aim is to study the properties of the cyanoacetylene molecule in a model potential which mimics the nanotubelike environment, we employ a two-dimensional harmonic potential centered at  $z$ -axis, along which the molecule was oriented in all calculations:

$$V_{\text{conf}} = \frac{1}{2}\varphi^2 r^2 = \frac{1}{2}\varphi^2(x^2 + y^2) \quad (1)$$

where  $\varphi$  is related to the quadratic force constant of the applied harmonic potential. The set of studied properties encompasses dipole moment ( $\mu$ ), polarizability ( $\alpha$ ), and first ( $\beta$ ) and second hyperpolarizabilities ( $\gamma$ ). These properties are defined as coefficients in a Taylor series expansion of the energy ( $E$ ) in an external electric field ( $F$ ) (using the Einstein summation notation):

$$E(F) = E(0) - \mu_i F_i - \frac{1}{2!} \alpha_{ij} F_i F_j - \frac{1}{3!} \beta_{ijk} F_i F_j F_k - \frac{1}{4!} \gamma_{ijkl} F_i F_j F_k F_l + \dots \quad (2)$$

$E(0)$  is the field-free energy. Except the imaginary part of second hyperpolarizability, the quantity related to the two-photon absorption process (see below), the frequency dependence of electric dipole properties is neglected in this study. In the case of polyatomic molecules, which require approximate treatments, one usually divides an electric-dipole property  $P$  into electronic ( $P^e$ ) and vibrational ( $P^{\text{vib}}$ ) contribution and determines these two separately:

$$P = P^e + P^{\text{vib}} \quad (3)$$

In the present study, we use the Romberg–Rutishauser (RR) scheme<sup>106</sup> to determine electronic contributions to longitudinal  $\mu$ ,  $\alpha$ ,  $\beta$ , and  $\gamma$  based on eq 2. In that event, we employed the electric field amplitudes  $\pm 2^n h$ , where  $h = 0.0002$  au and  $n = 0, 1, \dots, 6$ . The off-diagonal components were computed using the method proposed by Kurtz with the electric field amplitude equal to 0.001 au.<sup>107</sup> The isotropic averages of  $\alpha$  and  $\gamma$  and the vector component of  $\beta$  were calculated according to

$$\alpha_0 = \frac{1}{3} \sum_{i=x,y,z} \alpha_{ii} \quad (4)$$

$$\gamma_0 = \frac{1}{5} \sum_{i,j=x,y,z} \gamma_{iiii} \quad (5)$$

and

$$\beta_\mu = \sum_{i=x,y,z} \frac{\mu_i \beta_i}{|\mu|}, \quad \text{where } \beta_i = \frac{1}{5} \sum_{j=x,y,z} (\beta_{ijj} + \beta_{jij} + \beta_{jji}) \quad (6)$$

Electronic energies in the presence of double perturbation, that is the electric field and the confining potential  $E(F, \varphi)$ , were computed using the GAUSSIAN package<sup>108</sup> at several levels of theoretical approximation, including the Hartree–Fock, MP2, CCSD, and CCSD(T) methods.<sup>109–113</sup> In electron correlation methods, the 1s core orbitals of heavy atoms were kept frozen.

In this study we also consider the second-order transition moment in the presence of confining potential:

$$S_{ij}^{0 \rightarrow f} = \sum_n \left[ \frac{\langle 0 | \mu_i | n \rangle \langle n | \mu_j | f \rangle}{\omega_n - \frac{1}{2} \omega_f} + \frac{\langle 0 | \mu_j | n \rangle \langle n | \mu_i | f \rangle}{\omega_n - \frac{1}{2} \omega_f} \right] \quad (7)$$

which is directly related to the two-photon absorption strength, from the ground state  $|0\rangle$  to an excited state  $|f\rangle$ :<sup>114</sup>

$$\delta^{0 \rightarrow f} = \frac{1}{30} \sum_{ij} [S_{ii} S_{jj}^* F + S_{ij} S_{ij}^* G + S_{ij} S_{ji}^* H] \quad (8)$$

where  $F$ ,  $G$ , and  $H$  are polarization variables; in the case of linearly polarized photons  $F = G = H = 2$ . The effect of molecular vibrations on  $S^{0 \rightarrow f}$  is neglected in the present study; thus, the summation in eq 7 runs only over *electronic* states. In order to determine the  $S^{0 \rightarrow f}$  we employed the multireference configuration interaction wave function with single and double excitations and Davidson-type size extensivity corrections (MRCISD(Q))<sup>115</sup> with the reference configurations obtained by distributing six electrons in six  $\pi$  orbitals. In that case the summation was performed over 20 lowest-lying eigenvalues of a Hamiltonian. In the MRCISD(Q) calculations, we assumed the  $C_{2v}$  symmetry and hereafter we label excited states according to the energetic ordering in  $A_1$  representation. Calculations of  $S^{0 \rightarrow f}$  and spectroscopic parameters (excitation energies and transition moments) were performed using the MOLCAS programs.<sup>116,117</sup> The geometrical parameters of HCCCN molecule assumed in the above calculations were optimized at the CCSD/cc-pVTZ level approximation using the GAUSSIAN package.

In order to study the effect of spatial confinement on vibrational contributions to nonresonant electric-dipole properties, we employed the Bishop, Hasan, and Kirtman (BHK) variational approach.<sup>118,119</sup> The BHK method employs the finite-field nuclear relaxation (FF-NR) formalism to evaluate the vibrational nuclear relaxation (NR) (hyper)polarizabilities. The NR (hyper)polarizabilities includes all vibrational contributions



through first-order in mechanical and/or electrical anharmonicity and some of the second-order terms. The higher-order vibrational corrections, which are called curvature contributions, are usually smaller and also far more expensive to obtain; and therefore, they are not computed here.<sup>120,121</sup> In applying the FF-NR approach, geometry optimization has been performed while strictly maintaining the Eckart conditions.<sup>122</sup> Such optimizations were carried out with the aid of the procedure developed by Luis et al.<sup>123</sup> The numerical differentiation needed to evaluate the sum of electronic and NR contributions was performed with the Romberg–Rutishauser algorithm (applying the electric field amplitudes  $\pm 2^n h$ , where  $h = 0.0002$  au and  $n = 0, 1, \dots, 6$ ), thereby minimizing the contamination of higher power (in the field) terms.<sup>106</sup> The FF-NR treatment was applied only for the longitudinal (i.e., along  $z$ -axis) components of the static vibrational hyperpolarizabilities. For the confined HCCCN, the longitudinal tensor element of the electronic (hyper)polarizabilities is the dominant component. Except the calculations corresponding to  $\varphi = 0$  au which were done using the default algorithm available in GAUSSIAN program, all other geometry relaxations were performed using the Broyden–Fletcher–Goldfarb–Shanno method based on the numerical energy gradients also computed using the latter software.

All studied properties were calculated using the Dunning's correlation-consistent basis sets augmented with extra diffuse functions (aug-cc-pVDZ and aug-cc-pVTZ).<sup>124,125</sup>

## RESULTS AND DISCUSSION

In order to investigate the influence of spatial confinement on the electro-optic properties, we consider  $\varphi$  values of the external potential (see eq 1) in the range 0–0.32 au. The rationale behind selecting  $\varphi_{\max} = 0.32$  au follows from the analysis of interaction energy terms estimated for HCCCN molecule trapped inside carbon nanotubes of varying diameter. The total energy change due to the repulsive harmonic potential of cylindrical symmetry computed for  $\varphi_{\max}$  amounts to roughly the same magnitude as the exchange-repulsion between HCCCN molecule and the (3,3) SWCNT of  $\sim 0.45$  nm diameter (see the Supporting Information). Since the mean diameter of SWCNTs hosting experimentally studied polyynes was 1.4 nm,<sup>104</sup> the value of  $\varphi = 0.32$  au may be considered as a limiting case of the spatial confinement.

Unless otherwise indicated, the computations of  $\mu$ ,  $\alpha$ ,  $\beta$ ,  $\gamma$ , and  $S$  were performed at the equilibrium geometry, neglecting the effect of external potential on the position of nuclei. However, we attempted to estimate the effect of geometry relaxation in the case of most properties analyzed herein, including longitudinal components of  $\mu$ ,  $\alpha$ ,  $\beta$ , and  $\gamma$ . It should not be overlooked that the potential defined in eq 1 enters only the electronic part of the Hamiltonian, and then, the relaxation of nuclei is only indirect (i.e., due to the electron density reorganization in the presence of spatial confinement). The changes in geometrical parameters upon increasing value of  $\varphi$ , calculated at the CCSD/cc-pVTZ level, are presented in Table 1.

As seen, the spatial confinement leads to the shortening of all bonds. This is in line with the results of calculations reported by Klobukowski et al. for diatomic molecules<sup>44,90,92</sup> as well as those of Cammi et al. for 1,3-butadiene and diborane.<sup>126,127</sup> Particularly in the latter works, the authors argue that the observed shortening of the bond lengths may be interpreted as a consequence of the charge density deformation due to the Pauli repulsive interaction with the environment. The changes observed in this study do not exceed 0.005 Å up to  $\varphi = 0.08$  au

**Table 1. Changes in Bond Distances ( $\Delta_{i-j}$ , Given in Angstroms) with Respect to Geometry Optimized without the Presence of Confining Potential ( $\varphi = 0$ )<sup>a</sup>**

$\varphi$	$\Delta_{\text{H-C}_1}$	$\Delta_{\text{C}_1-\text{C}_2}$	$\Delta_{\text{C}_2-\text{C}_3}$	$\Delta_{\text{C}_3-\text{N}}$
0.08	−0.004	−0.004	−0.004	−0.003
0.16	−0.014	−0.016	−0.015	−0.013
0.24	−0.028	−0.032	−0.030	−0.027
0.32	−0.044	−0.049	−0.046	−0.042

<sup>a</sup>Calculations were performed using the CCSD/cc-pVTZ method.

and one immediately finds a general pattern for larger values of  $\varphi$ , i.e.:

$$|\Delta_{\text{C}_1-\text{C}_2}| > |\Delta_{\text{C}_2-\text{C}_3}| > |\Delta_{\text{H-C}_1}| > |\Delta_{\text{C}_3-\text{N}}|$$

Shortening of all bonds is accompanied by the increase of vibrational frequencies corresponding to axial stretching fundamentals (cf. Table 2). This trend is in line with the experimental results presented by Aoki et al.,<sup>128</sup> who studied pressure shifts of the internal frequencies of crystalline cyanoacetylene.

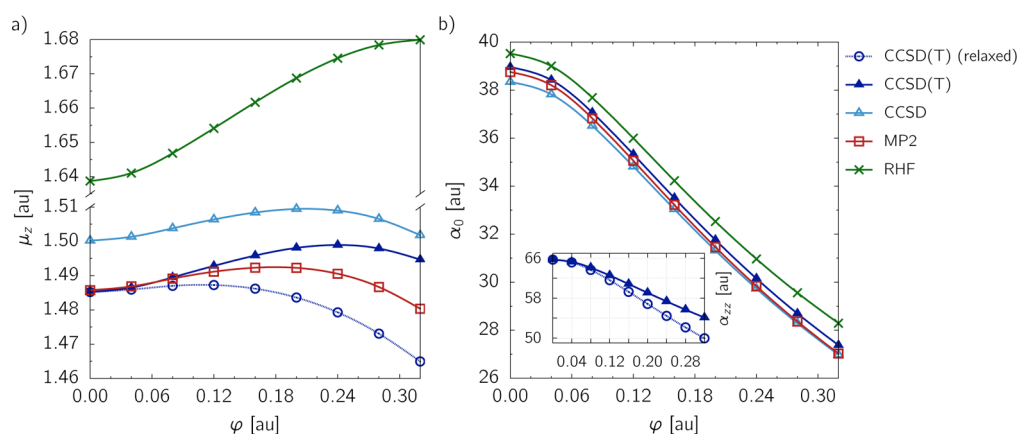
We would like to start the discussion of the electric properties of confined cyanoacetylene molecule with analysis of the results of nonresonant electric dipole properties, which are presented in Figures 1–3. Hereafter, we shall use  $\varphi$  and  $\varphi_{\max}$  to denote  $\varphi = 0$  and 0.32 au, respectively. The dipole moment of cyanoacetylene molecule is gradually increasing upon confinement as shown in Figure 1a. Interestingly, all of the employed electron correlation methods predict the maximum of  $\mu(\varphi)$  at some intermediate value of  $\varphi$  after which the magnitude of  $\mu$  starts decreasing. In the case of unrelaxed geometry, the higher the level of electron correlation treatment the larger the value of  $\varphi$  corresponding to  $\mu_{\max}(\varphi)$ . However, in the case of relaxed geometry,  $\mu_{\max}$  occurs for much smaller value of  $\varphi$  after which the magnitude of dipole moment drops significantly below that of a free molecule. Nonetheless, the largest relative change of dipole moment upon the spatial confinement does not exceed 2% for methods accounting for electron correlation. Still the possibility of altering the polarization upon confinement is quite intriguing. Our results shed also new light on the interpretation of Stark spectra of the HCCCN molecule in helium nanodroplets.<sup>95</sup> As it was mentioned in the Introduction, Stiles et al. have observed that the dipole moment of solvated HCCCN is slightly smaller (by roughly 4%) than in the gas-phase. Using a simple cavity model based on the concepts developed in physics of dielectrics, they demonstrated that this effect can be rationalized in terms of the dipole-induced polarization of helium atoms. On the other hand, our results indicate that the spatial confinement may also contribute to this effect, being either additional or perhaps even the main origin of this phenomenon. This conclusion is also supported by our earlier theoretical study on the electric properties of an HCCCN molecule embedded in helium nanotubelike cages,<sup>55</sup> as well as the experimentally observed blue-shifts of spectral lines of atoms in a liquid helium environment.<sup>129,130</sup>

Contrary to what has been observed in the case of dipole moment, the changes in polarizability values upon confinement are much more pronounced (cf. Figure 1b). Similarly as in the case of other molecules and atoms that have been studied so far, the isotropic average polarizability is substantially reduced upon confinement (see the discussion in the Introduction). The relative decrease of  $\alpha_0$  in the considered range of  $\varphi$  does not exceed 30% for the rigid geometry of HCCCN. However,

**Table 2.** Electronic and Nuclear Relaxation Contributions to Static Longitudinal (hyper)Polarizabilities (Given in Atomic Units) Computed at the Relaxed Geometries at the MP2/aug-cc-pVDZ Level of Theory<sup>a</sup>

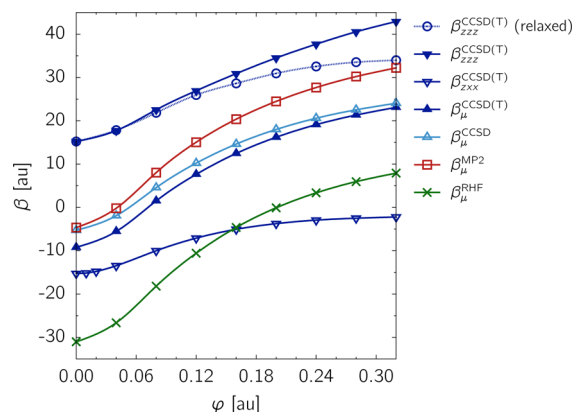
$\varphi$	$\alpha_{zz}^e(0; 0)$	$\alpha_{zz}^{NR}(0; 0)$	$\beta_{zzz}^e(0; 0, 0)$	$\beta_{zzz}^{NR}(0; 0, 0)$	$\gamma_{zzzz}^e(0; 0, 0, 0)$	$\gamma_{zzzz}^{NR}(0; 0, 0, 0)$	$\nu_4$	$\nu_3$	$\nu_2$
0.00	69.30	0.25	25.18	36.48	16919	8048	877	2002	2200
0.08	66.89	0.23	38.37	36.44	13727	7196	887	2024	2222
0.16	61.98	0.21	43.34	35.43	9927	5785	910	2080	2281

<sup>a</sup>The terms  $\nu_4$ – $\nu_2$  (given in inverse centimeters) are frequencies corresponding to stretching vibrations and were determined by the diagonalization of the mass-weighted hessian.

**Figure 1.** Electronic contributions to dipole moment (a) and isotropic average polarizability (b) of HCCCN molecule in the presence of the confining potential of cylindrical symmetry. Calculations were performed using the aug-cc-pVTZ basis set.

the effect of structural relaxation upon confinement leads to a much more rapid decrease of longitudinal polarizability  $\alpha_{zz}$  (see the inset of Figure 1b). Previously we have made a similar observation in the case of LiH molecule.<sup>51</sup> Virtually all employed methods predict the same effect and the major difference is only due to the small variations of the polarizabilities of a free molecule.

Much more intricate are the changes of first hyperpolarizability of the confined HCCCN molecule. A close inspection of Figure 2 presenting the results of computations of

**Figure 2.** Selected tensor elements and the vector component of first hyperpolarizability of HCCCN molecule in the presence of the confining potential of cylindrical symmetry. Calculations were performed using the aug-cc-pVTZ basis set.

the vector component of  $\beta$  in the direction of the permanent dipole moment ( $\beta_\mu$ , see eq 6) and the relevant tensor elements ( $\beta_{zzz}$  and  $\beta_{zxx} = \beta_{zyy}$ ) as a function of  $\varphi$  allows one to make a few interesting observations. First, the diagonal component  $\beta_{zzz}$  rises substantially upon increasing  $\varphi$  value and so does the  $\beta_\mu$

value. Upon confinement, the values of  $\beta_{zzz}$  grow up to almost three times their normal magnitude as the ratio of  $\beta_{zzz}(\varphi_{\max})$  to  $\beta_{zzz}(\varphi_0)$  amounts to 2.82 at the CCSD(T) level. Although the inclusion of structural relaxation quenches this effect to some extent, the  $\beta_{zzz}(\varphi_{\max})$  is still more than two times larger than that of a free molecule (the corresponding ratio computed at the CCSD(T) level is 2.23). Second, for  $\varphi_0$ , the off-diagonal components  $\beta_{zxx}$  and  $\beta_{zyy}$  are opposite in sign and of comparable absolute magnitude to  $\beta_{zzz}$ . Thus the resultant vector component of first hyperpolarizability is negative and amounts to  $-9.2$  au at the CCSD(T) level. However, the absolute magnitude of the off-diagonal components gradually diminishes for all considered values of  $\varphi$  and since this is accompanied by a significant increase of the diagonal component the  $\beta_\mu$  changes upon confinement from  $-9.2$  to  $23.1$  au. Thus even in terms of the absolute magnitude, the nonlinear response of HCCCN increases substantially in the presence of the confining potential of cylindrical symmetry. Finally, we note the poor performance of Hartree–Fock method which, as reported also by other authors,<sup>131,132</sup> has difficulty in predicting a correct sign of the first hyperpolarizability of organic compounds with the cyano groups. It should not be overlooked that the results of computations of  $\beta_{zzz}(\varphi)$  using the confining potential of cylindrical symmetry are in agreement with the previous results reported by some of us using the helium nanotube-like model.<sup>55</sup>

Figure 3 presents the influence of spatial confinement on the electronic contribution to the second hyperpolarizability, which is qualitatively similar to what has been found for  $\alpha_0$ . It follows from the plot that the isotropic average value of  $\gamma$  diminishes much more rapidly than the diagonal component  $\gamma_{zzzz}$  upon increasing strength of confinement (roughly by a factor of 2). Indeed, the CCSD(T) method predicts that  $\gamma_{zzzz}(\varphi_{\max})/\gamma_{zzzz}(\varphi_0) = 0.455$  and  $\gamma_0(\varphi_{\max})/\gamma_0(\varphi_0) = 0.238$ . This is a result of much more substantial quenching of the off-diagonal components of second hyperpolarizability in comparison with

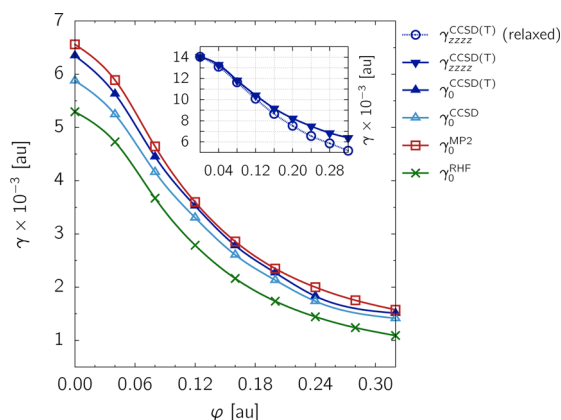


**Figure 3.** Diagonal tensor elements and the isotropic average second hyperpolarizability of HCCCN molecule in the presence of the confining potential of cylindrical symmetry. Calculations were performed using the aug-cc-pVTZ basis set.

the  $\gamma_{zzzz}$ . Similarly to what has been observed in the case of first hyperpolarizability, the Hartree–Fock approximation is unable to predict quantitatively the change of  $\gamma_0$  upon confinement; however, the shape of  $\gamma_0(\phi)$  determined using the CCSD(T) method is qualitatively reproduced.

Following our earlier study on the electric properties of the spatially restricted LiH molecule, we also made an attempt in the present work to assess the performance of selected exchange-correlation functionals in predicting these properties. The results of calculations of the longitudinal components of  $\mu$ ,  $\alpha$ ,  $\beta$ , and  $\gamma$  using the B3LYP, CAM-B3LYP, BLYP, LC-BLYP, M06, M06-2X, and PBE0 density functionals<sup>133–138</sup> are presented in the Supporting Information. As it turns out, there is no single functional which performs equally well in the case of all studied properties. The LC-BLYP functional is quite successful in predicting  $\alpha_{zz}$  and  $\beta_{zzzz}$  but it is the worst among all functionals in the case of  $\gamma_{zzzz}$  and  $\mu_z$ . Note the inability of all the employed functionals but LC-BLYP and M06 to correctly predict the sign of  $\beta_{zzzz}$  of a free molecule. The poor performance of density functionals comes as no surprise, since the electric-dipole properties of organic compounds with the cyano group are very sensitive to the description of electron correlation.<sup>139</sup> Nonetheless, all the studied functionals lead to a correct

semiquantitative description of the effect of the confinement on the (hyper)polarizabilities.

What we have seen in the case of static electronic second hyperpolarizability is that this quantity is quenched in the presence of spatial confinement. However, the opposite effect was found in the case of first hyperpolarizability. Thus, it is interesting to analyze the influence of spatial confinement on the diagonal component of the second-order transition moment tensor ( $S_{zz}$ ), which is related to the two-photon absorption strength  $\delta_{2PA}$ . In what follows, we shall analyze the  $S_{zz}$  corresponding to the two-photon absorption to the bright  $^1\Sigma^+$  electronic excited state. The gas-phase absorption spectrum of HCCCN recorded by Connors et al.<sup>100</sup> and more recently by Ferradaz et al.<sup>140</sup> shows several intense band systems extending between 165 and 110 nm. The first weaker band, which has been assigned to  $^1\Pi \leftarrow \tilde{X}$ , is followed by a strong valence transition with an origin at 145 nm (assigned to  $^1\Sigma^+ \leftarrow \tilde{X}$ ) and by a series of sharp Rydberg transitions converging to the first ionization potential at 107 nm (11.6 eV). Since the one-photon absorption spectrum of cyanoacetylene is well recognized,<sup>99,100,140–144</sup> we shall focus on the effect of confinement on the spectral features of the most intense  $^1\Sigma^+$  band and the corresponding second-order transition moment.

The results of calculations of  $S_{zz}$  in the presence of spatial confinement are presented in Figure 4a for the selected transitions within the  $^1A_1$  manifold, including the bright state  $^1\Sigma^+$  (being in the case of a free molecule the third excited state of  $A_1$  symmetry). Contrary to the static electronic second hyperpolarizability, the  $S_{zz}$  for the bright state increases upon confinement. The same is not true, however, for the neighboring  $^1\Sigma^+$  states, even though these are also  $\pi-\pi^*$  states of similar origin. Although the  $S_{zz}$  values for the other two states diminish with increasing strength of confinement, this change is relatively small. We should note that even though we discuss only the diagonal  $S_{zz}$  term, the results of our preliminary calculations of  $\delta_{2PA}$  employing the response formalism with MCSCF reference indicate that, indeed, the  $S_{zz}$  determines the shape of the  $\delta_{2PA}(\phi)$  function (see the Supporting Information).

In order to gain more insight into the origin of the observed increase of  $S_{zz}$  for the bright state, we derived from eq 7 a three-level model (TLM) including the ground state  $|0\rangle$  and two excited states: a final  $|f\rangle$  and an intermediate  $|n\rangle$  (in our case

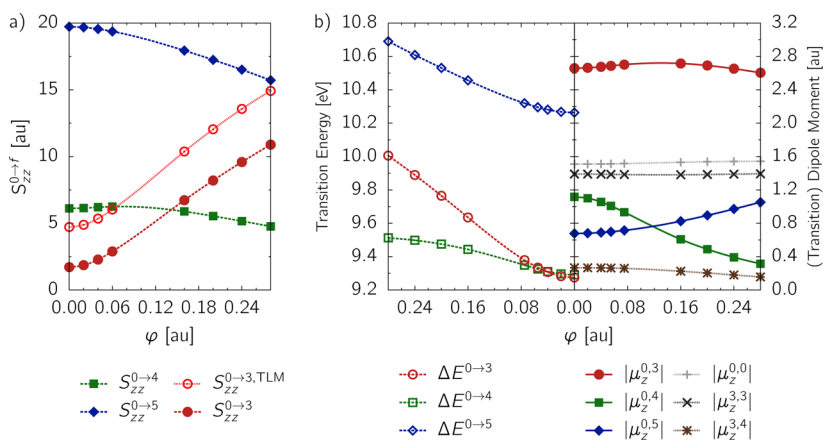


**Figure 4.** Diagonal component of second-order transition moment corresponding to the selected electronic transitions within  $^1A_1$  manifold (including the bright state  $^1\Sigma^+$  denoted as  $|3\rangle$ ) in the presence of the confining potential of cylindrical symmetry. Calculations were performed employing the MRCISD(Q) wave function and the aug-cc-pVTZ basis set. In the right panel, the corresponding spectroscopic parameters, i.e. the transition energies ( $\Delta E^{0 \rightarrow f}$ ) and the absolute values of (transition) dipole moments ( $\mu_z^{n,m}$ ) are shown.



these are the third and fourth excited states of  $^1A_1$  symmetry, respectively):

$$S_{zz}^{0 \rightarrow f, \text{TLM}} = 2 \left[ 2 \left( \frac{\langle 0|z|f \rangle [\langle f|z|f \rangle - \langle 0|z|0 \rangle]}{\omega_f} \right) + \frac{\langle 0|z|n \rangle \langle n|z|f \rangle}{\omega_n - \frac{1}{2}\omega_f} \right] \quad (9)$$

The estimated  $S_{zz}^{0 \rightarrow 3, \text{TLM}}$  shown in Figure 4a reproduces reasonably well the calculated  $S_{zz}^{0 \rightarrow 3}$  value. The dependence of the key parameters entering eq 9 on  $\varphi$  are shown in Figure 4b. It follows from this plot that the transition moment to the bright state ( $|3\rangle$ ) as well as the coupling term ( $\langle 3|z|4\rangle$ ) are virtually unaffected by the confining potential. Also the changes of excitation energy to the bright state do not alter the  $1/\omega_f$  factor in eq 9 significantly. Although it is not so obvious from the plot, a detailed analysis shows that the observed trend is in fact due to slight increase of  $\Delta\mu$  between the ground and the excited state that is multiplied by a large transition moment.

Finally, we come to the effect of spatial confinement on the vibrational (hyper)polarizabilities. Three decades ago, Bishop and Kirtman developed a perturbation method (BKPT) to compute the vibrational contributions to (hyper)polarizabilities. Although this method gives much insight into the electrical and mechanical anharmonicities through various orders of perturbation theory, we have not attempted to apply it here, as it requires evaluation of energy and property derivatives. As already mentioned, we use the FF-NR scheme to determine the vibrational hyperpolarizabilities under the spatial confinement. To the best of our knowledge, this aspect has not been addressed previously. In order to reduce the large computational cost connected with numerical evaluation of energy gradients in the presence of double perturbation ( $F, \varphi$ ), the FF-NR treatment was applied at the MP2/aug-cc-pVDZ level of theory. The results of calculations of nuclear-relaxation (hyper)polarizabilities, accompanied by the electronic contributions evaluated at the very same level of theory, are presented in Table 2. In the considered range of  $\varphi$  values, the rate of change of electronic and vibrational contribution to  $\alpha_{zz}$  is similar and in the case of the two counterparts one finds decrease. Likewise,  $\gamma_{zzzz}^e$  and  $\gamma_{zzzz}^{\text{NR}}$  decrease upon increasing spatial confinement, but the changes are much more noticeable. The latter quantity is less influenced by increasing values of  $\varphi$ . The most striking effect is found in the case of nuclear-relaxation first hyperpolarizability. In that event, substantial increase of  $\beta^e$  upon confinement is accompanied by only a small decrease of  $\beta^{\text{NR}}$ . The static NR first and second hyperpolarizabilities have the same order of magnitude than the corresponding static electronic properties and then cannot be neglected.

## SUMMARY AND OUTLOOK

Encapsulation of linear carbon molecules inside single-walled carbon nanotubes is a promising route to study their optical and electrical properties, as these compounds often are difficult to isolate. Stimulated by recent experimental studies on this subject, in this article we have made an attempt to elucidate the effect of the encapsulation on the molecular properties using high-level electron correlation treatments for a representative system—a cyanoacetylene molecule confined by repulsive potential of cylindrical symmetry, expected to capture the exchange repulsion within a carbon nanotube. The set of

studied properties include the electronic and vibrational (hyper)polarizabilities as well as the parameters characterizing one and the two-photon absorption spectra. Our results of calculations employing external potential demonstrate that the decrease in dipole moment observed experimentally by Stiles et al. for the HCCCN molecule solvated in helium nanodroplets may be partially attributed to the confinement effects. The results presented in this study also provide evidence that spatial confinement causes a substantial drop of the isotropic average polarizability and second hyperpolarizability. On the other hand, the vector component of first hyperpolarizability substantially increases upon confinement. Nuclear relaxation (hyper)polarizabilities are found to diminish upon confinement, albeit the magnitude of observed changes is quite different for first and second hyperpolarizability. The effect of structural relaxation on the electric-dipole properties, arising from the presence of the external potential, has also been addressed in the present work. It has been found that the spatial confinement leads to the shortening of all bonds accompanied by the increase of vibrational frequencies corresponding to axial stretching fundamentals. This trend is in line with the results of experimental study of pressure shifts of the internal frequencies of crystalline cyanoacetylene. Regarding the spectral features, our calculations indicate that the most intense  $^1\Sigma^+ \leftarrow \tilde{X}$  one-photon transition is slightly blue-shifted whereas the corresponding oscillator strength is virtually unaffected by the confinement. However, the absolute magnitude of the second-order transition moment for the bright state ( $S_{zz}^{0 \rightarrow ^1\Sigma^+}$ ) also increases with an increasing confinement even though it is slightly decreasing for neighboring  $^1\Sigma^+ \pi \rightarrow \pi^*$  states of similar origin.

In the present study, the maximum strength of spatial confinement was calibrated to mimic the exchange-repulsion between the HCCCN molecule and the (3,3) SWCNT of  $\sim 0.45$  nm diameter. In fact, the mean diameter of SWCNTs hosting experimentally studied polyynes was 1.4 nm.<sup>104</sup> Considering the rather weak sensitivity of parameters characterizing one-photon spectra (excitation energy, transition moments), our work indicates that the encapsulation of linear  $\pi$ -conjugated molecules in SWCNTs is a well-motivated tool to study their optical properties (provided that effects other than confinement also have not much influence on one-photon spectra). However, as far as electronic hyperpolarizabilities of encapsulated cyanoacetylene molecule are concerned, confinement effects in small-diameter SWNTs affect these properties to a large extent so that they lose their essential free-molecular character. An important finding of this study, of relevance for future theoretical considerations, is that the analytical confining potential approach as well as discrete helium-nanotube model provide a consistent picture of confinement effects as far as static electric-dipole properties are concerned. The former, however, has an advantage that it allows one to easily incorporate the effect of vibrations on (hyper)polarizabilities. To our knowledge, some of the studied topics, including the vibrational contributions to the electric properties and the two-photon absorption spectra of confined molecules, have never been considered in the literature and thorough studies on other polyatomic molecules are required to arrive at more general conclusions.

## ASSOCIATED CONTENT

### Supporting Information

Detailed justification of the range of applied confining potential strengths as well as the results illustrating performance of selected density functionals and the preliminary results of  $\delta_{2PA}$ .

This material is available free of charge via the Internet at <http://pubs.acs.org/>.

## AUTHOR INFORMATION

### Corresponding Author

\*E-mail: robert.gora@pwr.wroc.pl (R.W.G.); wojciech.bartkowiak@pwr.wroc.pl (W.B.).

### Notes

The authors declare no competing financial interest.

## ACKNOWLEDGMENTS

One of the authors (R.Z.) is a beneficiary of the KOLUMB fellowship funded by the Foundation for Polish Science (FNP). W.B. and R.W.G. are thankful for the financial support from the National Science Centre (Grant No. DEC-2011/01/D/ST4/03149). This work was also supported by a computational grant from Academic Computer Center CYFRONET AGH.

## REFERENCES

- (1) Schoonheydt, R. A.; Weckhuysen, B. M., Eds. *Molecules in confinement spaces: the interplay between spectroscopy and theory to develop structure-activity relationships in the field of heterogeneous catalysis, sorption, sensing and separation technology*. *Phys. Chem. Chem. Phys.* **2009**; Vol. 11, Special Issue, 2781–2992.
- (2) Song, Y.; Manaa, M. R., Eds. *Chemistry and materials science at high pressures symposium*. *J. Phys. Chem. C* **2012**; Vol. 116, Special Issue, 2059–2646.
- (3) McMahon, J. M.; Morales, M. A.; Pierleoni, C.; Ceperley, D. M. *Rev. Mod. Phys.* **2012**, 84, 1607–1653.
- (4) Bini, R.; Ceppatelli, M.; Citroni, M.; Schettino, V. *Chem. Phys.* **2012**, 398, 262–268.
- (5) Schettino, V.; Bini, R. *Chem. Soc. Rev.* **2007**, 36, 869–880.
- (6) Bini, R. *Acc. Chem. Res.* **2004**, 37, 95–101.
- (7) Gubbins, K. E.; Liu, Y.-C.; Moore, J. D.; Palmer, J. C. *Phys. Chem. Chem. Phys.* **2011**, 13, 58–85.
- (8) Grochala, W.; Hoffmann, R.; Feng, J.; Ashcroft, N. W. *Angew. Chem., Int. Ed.* **2007**, 46, 3620–3642.
- (9) Britz, D. A.; Khlobystov, A. N. *Chem. Soc. Rev.* **2006**, 35, 637–659.
- (10) Douhal, A. *Acc. Chem. Res.* **2004**, 37, 349–355.
- (11) Khlobystov, A. N.; Britz, D. A.; Briggs, G. A. D. *Acc. Chem. Res.* **2005**, 38, 901–909.
- (12) Sabin, J. R.; Brändas, E. J.; Cruz, S. A., Eds. *Advances in Quantum Chemistry: Theory of Confined Quantum Systems*; Academic Press: Waltham, MA, 2009; Vol. 57–58; pp 1–309.
- (13) Buchachenko, A. L. *J. Phys. Chem. B* **2001**, 105, 5839–5846.
- (14) Dolmatov, V.; Baltenkov, A.; Connerade, J.-P.; Manson, S. *Radiat. Phys. Chem.* **2004**, 70, 417–433.
- (15) Karwowski, J. *J. Mol. Struct.: THEOCHEM* **2005**, 727, 1–7.
- (16) Jaskólski, W. *Phys. Rep.* **1996**, 271, 1–66.
- (17) Connerade, J.-P.; Kengkan, P. *Proc. Idea-Finding Symposium*; Frankfurt Institute for Advanced Studies: Frankfurt, Germany, 2003; pp 35–46.
- (18) Ajami, D.; Rebek, J. *Acc. Chem. Res.* **2013**, 46, 990–999.
- (19) Caillier, C.; Machon, D.; San-Miguel, A.; Arenal, R.; Montagnac, G.; Cardon, H.; Kalbac, M.; Zukalova, M.; Kavan, L. *Phys. Rev. B* **2008**, 77, 125418.
- (20) Wang, S.; Yin, D.; Li, Z.; Yang, J. *J. Phys. Chem. Lett.* **2012**, 3, 2154–2158.
- (21) Michels, A.; de Boer, J.; Bijl, A. *Physica* **1937**, 4, 981–994.
- (22) Dalgarno, A.; Lewis, J. T. *Proc. R. Soc. A* **1957**, 240, 284–292.
- (23) Ley-Koo, E.; Rubinstein, S. *J. Chem. Phys.* **1979**, 71, 351–357.
- (24) LeSar, R.; Herschbach, D. R. *J. Phys. Chem.* **1983**, 87, 5202–5206.
- (25) Montgomery, H. E. *Chem. Phys. Lett.* **2002**, 352, 529–532.
- (26) Chattaraj, P.; Sarkar, U. *Chem. Phys. Lett.* **2003**, 372, 805–809.
- (27) Aquino, N.; Campoy, G.; Montgomery, H. E. *Int. J. Quantum Chem.* **2007**, 107, 1548–1558.
- (28) van Faassen, M. J. *Chem. Phys.* **2009**, 131, 104108.
- (29) Sarkar, U.; Khatua, M.; Chattaraj, P. K. *Phys. Chem. Chem. Phys.* **2012**, 14, 1716–1727.
- (30) Banerjee, A.; Sen, K. D.; Garza, J.; Vargas, R. J. *Chem. Phys.* **2002**, 116, 4054–4057.
- (31) Waugh, S.; Chowdhury, A.; Banerjee, A. *J. Phys. B: At. Mol. Opt. Phys.* **2010**, 43, 225002.
- (32) Sen, S.; Mandal, P.; Mukherjee, P. K. *Phys. Plasmas* **2012**, 19, 033501.
- (33) Saha, B.; Mukherjee, P. K.; Diercksen, G. H. F. *Astron. Astrophys.* **2002**, 396, 337–344.
- (34) Li, H.-W.; Kar, S. *Phys. Plasmas* **2012**, 19, 073303.
- (35) Li, H.-W.; Kar, S.; Jiang, P. *Int. J. Quantum Chem.* **2013**, 113, 1493–1497.
- (36) Ndengué, S. A.; Motapon, O. *J. Phys. B: At. Mol. Opt. Phys.* **2008**, 41, 045001.
- (37) Motapon, O.; Ndengue, S. A.; Sen, K. D. *Int. J. Quantum Chem.* **2011**, 111, 4425–4432.
- (38) Fowler, P. W.; Madden, P. A. *Phys. Rev. B* **1984**, 29, 1035–1042.
- (39) Fowler, P. W.; Madden, P. A. *Phys. Rev. B* **1985**, 31, 5443–5455.
- (40) Fowler, P. W.; Madden, P. A. *J. Phys. Chem.* **1985**, 89, 2581–2585.
- (41) Aguado, A.; Madden, P. A. *Phys. Rev. B* **2004**, 70, 245103.
- (42) Zhang, C.; Andersson, T.; Svensson, S.; Björneholm, O.; Huttula, M.; Mikkilä, M.-H.; Anin, D.; Tchapyguine, M.; Öhrwall, G. *J. Phys. Chem. A* **2012**, 116, 12104–12111.
- (43) Gorecki, J.; Byers Brown, W. J. *Chem. Phys.* **1988**, 89, 2138–2148.
- (44) Lo, J. M. H.; Klobukowski, M.; Bielińska-Wąz, D.; Schreiner, E. W. S.; Diercksen, G. H. F. *J. Phys. B: At. Mol. Opt. Phys.* **2006**, 39, 2385–2402.
- (45) Marin, J.; Muñoz, G. *J. Mol. Struct.: THEOCHEM* **1993**, 287, 281–285.
- (46) Mateos-Cortés, S.; Ley-Koo, E.; Cruz, S. A. *Int. J. Quantum Chem.* **2002**, 86, 376–389.
- (47) Lo, J.; Klobukowski, M. *Chem. Phys.* **2006**, 328, 132–138.
- (48) Cruz, S. A.; Soullard, J. *Chem. Phys. Lett.* **2004**, 391, 138–142.
- (49) Borgoo, A.; Tozer, D. J.; Geerlings, P.; De Proft, F. *Phys. Chem. Chem. Phys.* **2008**, 10, 1406–1410.
- (50) Bartkowiak, W.; Strasburger, K. *J. Mol. Struct.: THEOCHEM* **2010**, 960, 93–97.
- (51) Góra, R. W.; Zaleśny, R.; Kozłowska, J.; Naciążek, P.; Roztoczyńska, A.; Strasburger, K.; Bartkowiak, W. *J. Chem. Phys.* **2012**, 137, 094307.
- (52) Piela, L. *Ideas of quantum chemistry*, 1st ed.; Elsevier: New York, 2007; pp 743–744.
- (53) Papadopoulos, M. G.; Sadlej, A. J. *Chem. Phys. Lett.* **1998**, 288, 377–382.
- (54) Kędziera, D.; Avramopoulos, A.; Papadopoulos, M. G.; Sadlej, A. J. *Phys. Chem. Chem. Phys.* **2003**, 5, 1096–1102.
- (55) Kaczmarek, A.; Zaleśny, R.; Bartkowiak, W. *Chem. Phys. Lett.* **2007**, 449, 314–318.
- (56) Kaczmarek, A.; Bartkowiak, W. *Phys. Chem. Chem. Phys.* **2009**, 11, 2885–2892.
- (57) Małolepsza, E.; Piela, L. *Collect. Czech. Chem. Commun.* **2003**, 68, 2344–2354.
- (58) Małolepsza, E.; Piela, L. *J. Phys. Chem. A* **2003**, 107, 5356–5360.
- (59) Munn, R.; Malagoli, M.; in het Panhuis, M. *Synt. Met.* **2000**, 109, 29–32.
- (60) Munn, R.; Petelenz, P. *Chem. Phys. Lett.* **2004**, 392, 7–10.
- (61) Mennucci, B.; Amovilli, C.; Tomasi, J. *Chem. Phys. Lett.* **1998**, 286, 221–225.
- (62) Bartkowiak, W. In *Non-linear optical properties of matter: from molecules to condensed phases*; Papadopoulos, M. G., Sadlej, A. J., Leszczynski, J., Eds.; Springer: New York, 2006; pp 299–318.
- (63) Ramachandran, C.; Fazio, D. D.; Sathyamurthy, N.; Aquilanti, V. *Chem. Phys. Lett.* **2009**, 473, 146–150.



- (64) Besley, N. A.; Noble, A. J. *Chem. Phys.* **2008**, *128*, 101102.
- (65) Kaczmarek-Kędziera, A. J. *Phys. Chem. A* **2011**, *115*, 5210–5220.
- (66) Ma, F.; Zhou, Z.-J.; Liu, Y.-T. *ChemPhysChem* **2012**, *13*, 1307–1312.
- (67) Ensing, B.; Costanzo, F.; Silvestrelli, P. L. *J. Phys. Chem. A* **2012**, *116*, 12184–12188.
- (68) Kaczor, A.; Reva, I.; Fausto, R. *J. Phys. Chem. A* **2013**, *117*, 888–897.
- (69) Zhou, X.; Wesolowski, T. A.; Tabacchi, G.; Fois, E.; Calzaferri, G.; Devaux, A. *Phys. Chem. Chem. Phys.* **2013**, *15*, 159–167.
- (70) Fradelos, G.; Wesolowski, T. A. *J. Phys. Chem. A* **2011**, *115*, 10018–10026.
- (71) García, G.; Ciofini, I.; Fernández-Gómez, M.; Adamo, C. *J. Phys. Chem. Lett.* **2013**, *4*, 1239–1243.
- (72) Korona, T.; Hesselmann, A.; Dodziuk, H. *J. Chem. Theory Comput.* **2009**, *5*, 1585–1596.
- (73) Korona, T.; Dodziuk, H. *J. Chem. Theory Comput.* **2011**, *7*, 1476–1483.
- (74) Hesselmann, A.; Korona, T. *Phys. Chem. Chem. Phys.* **2011**, *13*, 732–743.
- (75) Podeszwa, R.; Cencek, W.; Szalewicz, K. *J. Chem. Theory Comput.* **2012**, *8*, 1963–1969.
- (76) Eriksen, J. J.; Sauer, S. P. A.; Mikkelsen, K. V.; Christiansen, O.; Jensen, H. J. A.; Kongsted, J. *Mol. Phys.* **2013**, DOI: 10.1080/00268976.2013.793841.
- (77) Skwara, B.; Góra, R. W.; Zaleśny, R.; Lipkowski, P.; Bartkowiak, W.; Reis, H.; Papadopoulos, M. G.; Luis, J. M.; Kirtman, B. *J. Phys. Chem. A* **2011**, *115*, 10370–10381.
- (78) Marquez, C.; Nau, W. M. *Angew. Chem., Int. Ed.* **2001**, *40*, 4387–4390.
- (79) Zhang, J.; Bearden, D. W.; Fuhrer, T.; Xu, L.; Fu, W.; Zuo, T.; Dorn, H. C. *J. Am. Chem. Soc.* **2013**, *135*, 3351–3354.
- (80) Yu, J.; Cui, Y.; Wu, C.; Yang, Y.; Wang, Z.; O’Keeffe, M.; Chen, B.; Qian, G. *Angew. Chem., Int. Ed.* **2012**, *51*, 10542–10545.
- (81) Suzuki, Y.; Tenma, Y.; Nishioka, Y.; Kawamata, J. *Chem. Asian J.* **2012**, *7*, 1170–1179.
- (82) Kamada, K.; Tanamura, Y.; Ueno, K.; Ohta, K.; Misawa, H. *J. Phys. Chem. C* **2007**, *111*, 11193–11198.
- (83) Yang, G.; Li, Y.; Dreger, Z.; White, J.; Drickamer, H. *Chem. Phys. Lett.* **1997**, *280*, 375–380.
- (84) Li, Y.; Yang, G.; Dreger, Z. A.; White, J. O.; Drickamer, H. G. *J. Phys. Chem. B* **1998**, *102*, 5963–5968.
- (85) Dreger, Z. A.; Yang, G.; White, J. O.; Drickamer, H. G. *J. Phys. Chem. A* **1997**, *101*, 5753–5757.
- (86) Dreger, Z. A.; Yang, G.; White, J. O.; Li, Y.; Drickamer, H. G. *J. Phys. Chem. A* **1997**, *101*, 9511–9519.
- (87) Dreger, Z. A.; Yang, G.; White, J. O.; Li, Y.; Drickamer, H. G. *J. Phys. Chem. B* **1998**, *102*, 4380–4385.
- (88) Patil, S.; Varshni, Y. Properties of confined hydrogen and helium atoms. In *Advances in Quantum Chemistry: Theory of Confined Quantum Systems—Part One*; Sabin, J. R., Brändas, E. J., Eds.; Academic Press: Waltham, MA, 2009; Vol. 57; pp 1–24.
- (89) Taut, M. *Phys. Rev. A* **1993**, *48*, 3561–3566.
- (90) Lo, J. M.; Klobukowski, M.; Dierksen, G. H. Low-lying excited states of the hydrogen molecule in cylindrical harmonic confinement. In *Advances in Quantum Chemistry*; Sabin, J., Ed.; Academic Press: Waltham, MA, 2005; Vol. 48; pp 59–89.
- (91) Sako, T.; Yamamoto, S.; Dierksen, G. H. F. *J. Phys. B: At. Mol. Opt. Phys.* **2004**, *37*, 1673–1688.
- (92) Lo, J. M. H.; Klobukowski, M.; Bielińska-Wąż, D.; Dierksen, G. H. F.; Schreiner, E. W. S. *J. Phys. B: At. Mol. Opt. Phys.* **2005**, *38*, 1143–1159.
- (93) Heidari, I.; Val, N.; Pal, S.; Kanhere, D. *Chem. Phys. Lett.* **2013**, *555*, 263–267.
- (94) Castro, L.; Castro, A. *J. Math. Chem.* **2013**, *51*, 265–277.
- (95) Stiles, P. L.; Nauta, K.; Miller, R. E. *Phys. Rev. Lett.* **2003**, *90*, 135301.
- (96) Turner, B. E. *Astrophys. J.* **1971**, *163*, L35–L39.
- (97) Bockelée-Morvan, D.; Lis, D.; Wink, J.; Despois, D.; Crovisier, J.; Bachiller, R.; Benford, D.; Biver, N.; Colom, P.; Davies, J.; Gérard, E.; Germain, B.; Houde, M.; Mehringer, D.; Moreno, R.; Paubert, G.; Phillips, T.; Rauer, H. *Astron. Astrophys.* **2000**, *353*, 1101–1114.
- (98) Kunde, V. G.; Aikin, A. C.; Hanel, R. A.; Jennings, D. E.; Maguire, W. C.; Samuelson, R. E. *Nature* **1981**, *292*, 686–688.
- (99) Vieira Mendes, L. A.; Boyé-Péronne, S.; Jacovella, U.; Liévin, J.; Gauyacq, D. *Mol. Phys.* **2012**, *110*, 2829–2842.
- (100) Connors, R. E.; Roebber, J. L.; Weiss, K. *J. Chem. Phys.* **1974**, *60*, S011–S024.
- (101) Topic, W.; Jäger, W.; Blinov, N.; Roy, P.-N.; Botti, M.; Moroni, S. *J. Chem. Phys.* **2006**, *125*, 144310.
- (102) Sun, X.; Hu, Y.; Zhu, H. *Chem. Phys. Lett.* **2013**, *566*, 4–7.
- (103) Nishide, D.; Dohi, H.; Wakabayashi, T.; Nishibori, E.; Aoyagi, S.; Ishida, M.; Kikuchi, S.; Kitaura, R.; Sugai, T.; Sakata, M.; Shinohara, H. *Chem. Phys. Lett.* **2006**, *428*, 356–360.
- (104) Nishide, D.; Wakabayashi, T.; Sugai, T.; Kitaura, R.; Kataura, H.; Achiba, Y.; Shinohara, H. *J. Phys. Chem. C* **2007**, *111*, 5178–5183.
- (105) Malard, L. M.; Nishide, D.; Dias, L. G.; Capaz, R. B.; Gomes, A. P.; Jorio, A.; Achete, C. A.; Saito, R.; Achiba, Y.; Shinohara, H.; Pimenta, M. A. *Phys. Rev. B* **2007**, *76*, 233412.
- (106) Medved’, M.; Stachová, M.; Jacquemin, D.; André, J.-M.; Perpète, E. A. *J. Mol. Struct.: THEOCHEM* **2007**, *847*, 39–46.
- (107) Kurtz, H. A.; Stewart, J. J. P.; Dieter, K. M. *J. Comput. Chem.* **1990**, *11*, 82–87.
- (108) Frisch, M. J.; Trucks, G. W.; Schlegel, H. B.; Scuseria, G. E.; Robb, M. A.; Cheeseman, J. R.; Scalmani, G.; Barone, V.; Mennucci, B.; Petersson, G. A.; Nakatsuji, H.; Caricato, M.; Li, X.; Hratchian, H. P.; Izmaylov, A. F.; Bloino, J.; Zheng, G.; Sonnenberg, J. L.; Hada, M.; Ehara, M.; Toyota, K.; Fukuda, R.; Hasegawa, J.; Ishida, M.; Nakajima, T.; Honda, Y.; Kitao, O.; Nakai, H.; Vreven, T.; Montgomery, J.; Peralta, J. E.; Ogliaro, F.; Bearpark, M.; Heyd, J. J.; Brothers, E.; Kudin, K. N.; Staroverov, V. N.; Kobayashi, R.; Normand, J.; Raghavachari, K.; Rendell, A.; Burant, J. C.; Iyengar, S. S.; Tomasi, J.; Cossi, M.; Rega, N.; Millam, J. M.; Klene, M.; Knox, J. E.; Cross, J. B.; Bakken, V.; Adamo, C.; Jaramillo, J.; Gomperts, R.; Stratmann, R. E.; Yazyev, O.; Austin, A. J.; Cammi, R.; Pomelli, C.; Ochterski, J. W.; Martin, R. L.; Morokuma, K.; Zakrzewski, V. G.; Voth, G. A.; Salvador, P.; Dannenberg, J. J.; Dapprich, S.; Daniels, A. D.; Farkas, O.; Foresman, J. B.; Ortiz, J. V.; Cioslowski, J.; Fox, D. J. *Gaussian 09*, revision C.01. 2009; Gaussian Inc.: Wallingford CT.
- (109) Roothaan, C. C. J. *Rev. Mod. Phys.* **1951**, *23*, 69–89.
- (110) Møller, C.; Plesset, M. S. *Phys. Rev.* **1934**, *46*, 618–622.
- (111) Čížek, J. On the Use of the Cluster Expansion and the Technique of Diagrams in Calculations of Correlation Effects in Atoms and Molecules. In *Advances in Chemical Physics: Correlation Effects in Atoms and Molecules*; LeFebvre, R., Moser, C., Eds.; John Wiley & Sons, Inc.: Hoboken, NJ, 1969; Vol. 14, p 35–89.
- (112) Scuseria, G. E.; Janssen, C. L.; Schaefer, H. F. *J. Chem. Phys.* **1988**, *89*, 7382–7387.
- (113) Raghavachari, K.; Trucks, G. W.; Pople, J. A.; Head-Gordon, M. *Chem. Phys. Lett.* **1989**, *157*, 479–483.
- (114) Monson, P. R.; McClain, W. M. *J. Chem. Phys.* **1970**, *53*, 29–37.
- (115) Langhoff, S. R.; Davidson, E. R. *Int. J. Quantum Chem.* **1974**, *8*, 61–72.
- (116) Aquilante, F.; De Vico, L.; Ferre, N.; Ghigo, G.; Malmqvist, P.-A.; Neogrady, P.; Pedersen, T. B.; Pitonak, M.; Reiher, M.; Roos, B. O.; Serrano-Andres, L.; Urban, M.; Veryazov, V.; Lindh, R. *J. Comput. Chem.* **2010**, *31*, 224–247.
- (117) Karlström, G.; Lindh, R.; Malmqvist, P.-A.; Roos, B. O.; Ryde, U.; Veryazov, V.; Widmark, P.-O.; Cossi, M.; Schimmelpennig, B.; Neogrady, P.; Seijo, L. *Comput. Mater. Sci.* **2003**, *28*, 222–239.
- (118) Bishop, D. M.; Hasan, M.; Kirtman, B. *J. Chem. Phys.* **1995**, *103*, 4157–4159.
- (119) Kirtman, B.; Luis, J. M.; Bishop, D. M. *J. Chem. Phys.* **1998**, *108*, 10008–10012.
- (120) Torrent-Sucarrat, M.; Solà, M.; Duran, M.; Luis, J. M.; Kirtman, B. *J. Chem. Phys.* **2002**, *116*, 5363–5373.

- (121) Torrent-Sucarrat, M.; Solà, M.; Duran, M.; Luis, J. M.; Kirtman, B. *J. Chem. Phys.* **2004**, *120*, 6346–6355.
- (122) Eckart, C. *Phys. Rev.* **1926**, *28*, 711–726.
- (123) Luis, J. M.; Duran, M.; Andrés, J. L.; Champagne, B.; Kirtman, B. *J. Chem. Phys.* **1999**, *111*, 875–884.
- (124) Dunning, T. H. *J. Chem. Phys.* **1989**, *90*, 1007–1023.
- (125) Kendall, R. A.; Dunning, T. H.; Harrison, R. J. *J. Chem. Phys.* **1992**, *96*, 6796–6806.
- (126) Cammi, R.; Verdolino, V.; Mennucci, B.; Tomasi, J. *Chem. Phys.* **2008**, *344*, 135–141.
- (127) Cammi, R.; Cappelli, C.; Mennucci, B.; Tomasi, J. *J. Chem. Phys.* **2012**, *137*, 154112.
- (128) Aoki, K.; Kakudate, Y.; Yoshida, M.; Usuba, S.; Fujiwara, S. *J. Chem. Phys.* **1989**, *91*, 2814–2817.
- (129) Tabbert, B.; Günther, H.; Putlitz, G. *J. Low Temp. Phys.* **1997**, *109*, 653–707.
- (130) Modesto-Costa, L.; Coutinho, K.; Mukherjee, P. K.; Canuto, S. *Chem. Phys. Lett.* **2012**, *533*, 25–29.
- (131) Jacquemin, D.; André, J.-M.; Perpète, E. A. *J. Chem. Phys.* **2004**, *121*, 4389–4396.
- (132) Suponitsky, K. Y.; Tafur, S.; Masunov, A. E. *J. Chem. Phys.* **2008**, *129*, 044109.
- (133) Becke, A. D. *J. Chem. Phys.* **1993**, *98*, 5648–5652.
- (134) Lee, C.; Yang, W.; Parr, R. G. *Phys. Rev. B* **1988**, *37*, 785–789.
- (135) Yanai, T.; Tew, D. P.; Handy, N. C. *Chem. Phys. Lett.* **2004**, *393*, 51–57.
- (136) Iikura, H.; Tsuneda, T.; Yanai, T.; Hirao, K. *J. Chem. Phys.* **2001**, *115*, 3540–3544.
- (137) Perdew, J. P.; Burke, K.; Ernzerhof, M. *Phys. Rev. Lett.* **1996**, *77*, 3865–3868.
- (138) Zhao, Y.; Truhlar, D. *Theor. Chem. Acc.* **2008**, *120*, 215–241.
- (139) Baranowska-Łączkowska, A.; Bartkowiak, W.; Góra, R. W.; Pawłowski, F.; Zaleśny, R. *J. Comput. Chem.* **2013**, *34*, 819–826.
- (140) Ferradaz, T.; Bénilan, Y.; Fray, N.; Jolly, A.; Schwell, M.; Gazeau, M.; Jochims, H.-W. *Planet. Spc. Sci.* **2009**, *57*, 10–22.
- (141) Job, V.; King, G. *J. Mol. Spectrosc.* **1966**, *19*, 155–177.
- (142) Job, V.; King, G. *J. Mol. Spectrosc.* **1966**, *19*, 178–184.
- (143) Seki, K.; He, M.; Liu, R.; Okabe, H. *J. Phys. Chem.* **1996**, *100*, 5349–5353.
- (144) Titarchuk, T.; Halpern, J. B. *Chem. Phys. Lett.* **2000**, *323*, 305–311.